Microbial consortia in salt marsh sediments are sequentially buried over millennia and genomic complementarity analysis indicates an important role in complex carbon decomposition

Joseph H. Vineis[1,2], Ashley N. Bulseco[1,3], Zoe G. Cardon[2], and Jennifer L. Bowen[1]

[1]Marine Science Center, Northeastern University, Nahant, Massachusetts, USA

[2]The Ecosystems Center, Marine Biological Laboratory, Woods Hole, Massachusetts, USA

[3]Department of Biological Sciences, University of New Hampshire, Durham, New Hampshire, USA

Abstract (250 words)

Salt marsh sediments contain high levels of microbial diversity and functions that reflect the heterogeneity of available nutrients, dynamic hydrology, and layers of organic matter developed over millennia. However, the microbially mediated processes involved in the cycling of complex carbon are still largely undescribed. We used genome reconstruction, co-occurrence networks, and genome scale metabolic modeling to identify the functional capacity for organic matter decomposition and transformation among groups of co-occurring microbes from 5-240 cm of sediment in a *Spartina patens* salt marsh, representing over 2000 years of sediment accumulation. We identified four consortia with similar taxonomic and functional profiles, but distinctly different distributions within the sedimentary layers. Microbial members common to each of these consortia included novel members of Bathyarchaeia BA1, Desulfatiglandales, Chloroflexota, Caldatribacteriota (JS1), Planctomycetota, and WOR3. The collective metabolic potential of these core consortia contained the capacity to decompose complex carbon and aromatics through syntrophic interactions. The composition and

functional potential of these co-occurring members are most similar to communities inhabiting sediment hundreds of meters beneath the surface of deep-sea sediments. Our results suggest that the assembly of communities within the salt marsh sediment are similarly governed by burial and nutrient limitation. The burial processes and putative syntrophy identified here provide a mechanistic understanding of how microbial life can persist under energy limited conditions and contribute to the transformation of carbon within salt marsh sediment.

Keywords: *Spartina alterniflora*, salt marsh sediment, syntrophy, consortia, acetogens, aromatic carbon, Wood-Ljungdahl

Introduction

Salt marshes are globally important to carbon storage and have the potential to influence both the changing climate and the stability of coastal systems. Salt marsh sediments contain between 400 – 6500 Tg of organic carbon (McLeod et al 2011, Duarte et al 2013, Temminik et al 2022) and store an additional 10.2 - 44.6 Mt annually, the equivalent of 0.5-1.0% of anthropogenic C emissions (Chmura et al 2003, Ouygang and Lee 2014). However, carbon storage in salt marshes is declining and estimates indicate that over a recent nine-year period, salt marsh habitat loss resulted in emission of 16.3 Tg of CO_2 and a reduction of 0.045 Tg of CO_2 burial per year (Campbell et al. 2022).

Rapidly increasing sea level rise and warming climate could destabilize current stocks of organic carbon with unpredictable consequences (Fontaine et al. 2007; Spivak

et al. 2019). Microbial communities within salt marsh sediments are compositionally and metabolically diverse and their interactions influence pools of soil organic carbon (SOC) (Bulseco et al. 2019; Erb, Keiser, and DeAngelis 2024). However, there are important knowledge gaps in our understanding of the metabolic capacity and distribution of microbial communities in blue carbon systems. Salt marsh sediments are generally unexplored, and studies of this system often lead to the identification of previously unidentified carbon cycling among novel taxa (Payne et al. 2025; Seitz et al. 2016). Identifying how the pools of carbon are influenced by microbial communities will enhance our understanding of the fate of blue carbon stocks, how they are formed, and how they change over time.

The decomposition of organic material is strongly influenced by plant communities that blanket the surface of the marsh in nearly homogenous stands. The regions of the marsh inhabited by plants are highly dynamic zones that contain hot spots of microbial activity due to plant-microbial interactions and feedbacks that are sensitive to seasonal and tidal influence (Kuzyakov and Blagodatskaya 2015). *Spartina patens* is a highly productive salt marsh macrophyte with roots that release organic carbon and aerate the sediment, thereby influencing carbon sequestration of salt marshes through the “microbial carbon pump” (Liang, Schimel, and Jastrow 2017; Spivak et al. 2019). Live roots of *S. patens* are dominantly 0-10cm below the sediment surface (Gallagher and Plumley 1979) and plant inputs could influence the SOC pool up to 100 cm deep (Liu et al. 2017). Microbial communities within this dynamic region of the sediment are also supported by non-plant derived sources of carbon, such as benthic microalgae (Boschker, De Brouwer, and Cappenberg 1999).

The patchy distribution of resources and dynamic processes in marsh sediments present challenges for unraveling the underlying rules for community assembly and metabolism. Identifying the distribution and putative functions of the microbial genomes within the dynamic zone influenced by plants and tidal inputs remains one of the most challenging but critical aspects to understanding the carbon and nutrient cycling in salt marsh systems. While decomposition within the salt marsh is conducted primarily by sulfate reducers (Howes, Dacey, and King 1984), most of the alternative pathways for anaerobic respiration, fermentation, and carbon fixation pathways have also been identified in marsh sediments (Baker et al. 2015a; Vineis, Bulseco, and Bowen 2023) and we are only beginning to understand how many of the carbon cycling processes are linked among organisms and within individual genomes.

Below the rooting zone and beyond the influence of living plants, salt marshes have accumulated vast stores of organic peat that date back, in some cases, millennia (Kirwan et al. 2023). These older sediments are likely to contain microbes adapted to survive in the deep, low energy environment (Bulseco et al. 2020) where prior oxidation of organic material has led to a decline in the bioavailability of organic carbon with sediment age and depth (Arndt et all 2013). Microbial communities below the influence of living plants therefore might mirror other marine low energy sediment communities supported by complex organic matter derived from compounds such as lignin, cellulose, and phenolic polymers (Arndt et al. 2013; Jørgensen and Boetius 2007). Decomposition of these compounds within energy limited sediment is often dependent on syntrophic interactions among microbial consortia (Peng et al, 2023). The specific mechanism of microbial decomposition has important consequences for carbon stability

because microbial turnover can result in the production of carbon that is protected from further decomposition (Liang et al. 2017). Therefore, identifying the capacity for microbial decomposition is important to understanding the susceptibility of long-term carbon storage within salt marsh sediments.

The physical and biogeochemical differences between the dynamic upper layers of the sediment, the energy poor deeper layers, and the transition between the two environments, are likely to support distinctly different microbial communities. We hypothesize that communities within dynamic upper layers will contain genomes with diverse functional potential. Additionally, we hypothesize that the energy limited deeper regions of the sediment will contain microbial consortia assembled to efficiently metabolize complex carbon. We aim to identify the boundaries of both metabolically flexible genomes and those relying on metabolic handoffs. We also consider the possibility that compositional changes in these low energy sediments will mirror the burial processes observed in marine environments that contain similar energetic limitations (Kirkpatrick, Walsh, and D'Hondt 2019; Walsh et al. 2016).

To test these hypotheses, we evaluated the structure and potential function of microbial communities within 5-240 cm depth fractions from two *S. patens* salt marshes, using a genomic lens. We evaluated the microbial community phylogenetic and community distribution and co-occurrence. We also characterized the functional capacity of genomes to identify their potential role in carbon transformation and decomposition. Finally, we constructed genome-scale metabolic models (GEMs) among co-occurring microbial genomes to identify potential functional complementarity important to carbon cycling.

Methods

1. Sampling

Six sediment cores were taken using a Russian peat corer from the salt marsh platform at two sites in Rowley MA, USA (42.759 N, 70.891 W) primarily vegetated by *Spartina patens*. The sites are part of the Plum Island Ecosystem (PIE) Long-Term Ecological Research site (LTER). Three cores were collected from the high marsh *Spartina patens* platform at two adjacent creeks, West and Sweeney Creek (Fig. 1), and a detailed description including biogeochemistry of the cores have been previously described (Bulseco-McKim 2018). The two creeks are approximately 2 km apart and cores taken within the marsh at each creek were separated by less than 50 meters (Fig. 1). Cores were sampled up to 240 cm, representing approximately 3000 yr old sediment . Subsections were collected approximately every 10 cm (Fig. 1). Sediment within each 2 cm sub-section was homogenized in a sterile 50 mL falcon tube and subsamples were flash frozen using liquid nitrogen and then stored at -80°C for nucleic acid analysis.

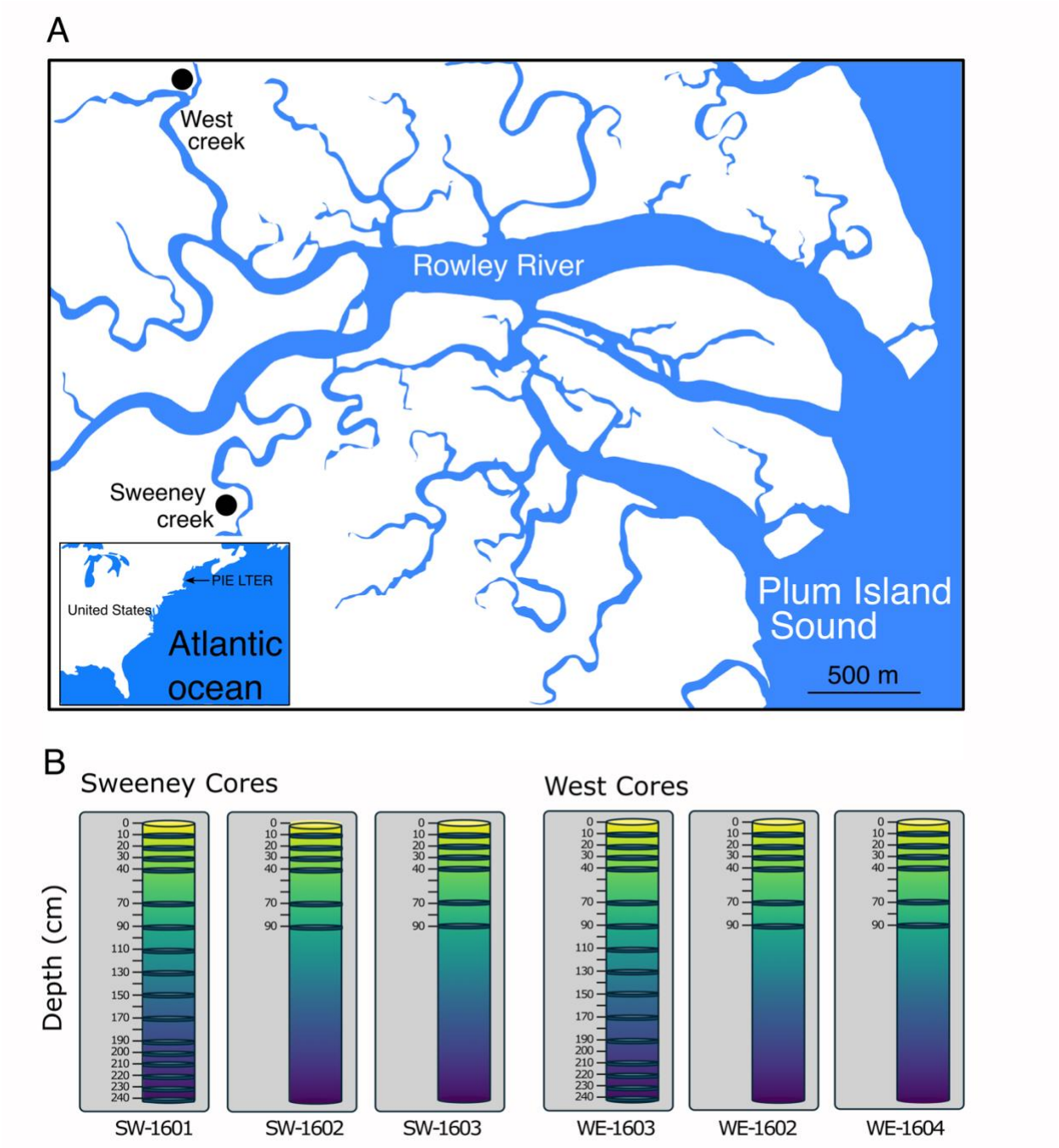

Figure 1. A) Map of the coring locations within the Plum Island Estuary Long Term Ecological Research (PIE LTER) site and B) the sample depth increments collected from each of the six cores.

142 **2. Metagenomic Sequencing**

143 The input DNA for sequencing library construction was extracted from
144 homogenized sediment from each 2 cm thick fraction (0.25 g wet weight) using a
145 Qiagen Power Soil DNA extraction kit (Qiagen, Germantown, MD) according to the
146 manufacturer's recommendations. We evaluated the quality and the quantity of DNA
147 using a Nanodrop and Quant-IT DNA assay (Invitrogen, USA) respectively. Purified
148 DNA was shipped overnight to the Joint Genome Institute (JGI) on dry ice. At JGI,
149 libraries were created using paired-end (PE) library construction with an insert size of
150 250 bp. Each library was uniquely barcoded and sequenced according to PE 2x151
151 chemistry on an Illumina NovaSeq. Sequences were quality filtered using the default
152 settings of BBTools v38.26 at JGI (Bushnell 2021). Quality filtered sequences of each
153 sample were independently assembled using SPAdes assembler 3.12.0 (Bankevich et
154 al. 2012).

155

156 **3. MAG reconstruction, dereplication, phylogenomics and metagenomic read**
157 **recruitment**

158 We used assemblies and quality filtered sequences generated by JGI/IMG for
159 each of the 55 samples to reconstruct metagenome-assembled genomes (MAGs) for
160 each independent sample. The assembled MAGs represent a population of cells.
161 Therefore, we refer to MAGs as populations or population genomes. Genome
162 reconstruction efforts can be improved by co-assembly of multiple samples in a gradient
163 or time series, especially when read counts are not sufficient to provide the minimum
164 amount of coverage necessary for assembly (Baker et al. 2015b; Stewart et al. 2018).

165 However, the detection of redundant MAGs across samples requires that genome
166 reconstruction be carried out for each sample independently and the number of high-
167 quality genomes recovered can be improved by reconstructing genomes from individual
168 samples compared to a single co-assembly (Olm et al. 2017).

169 We reconstructed draft genomes for each sample using CONCOCT (Alneberg et
170 al. 2014) as an automated guide for genome binning, followed by manual curation of
171 each CONCOCT MAG in Anvi'o, using contig tetranucleotide frequency, coverage,
172 taxonomic assignment, completion, and contamination to guide this process (Eren et al.
173 2015, 2021). In cases where the placement of contigs could not be resolved among a
174 group of similar MAGs, we used anvi-refine to provide increased resolution on this
175 subset of similar MAGs. This allowed for the separation of closely related MAGs and/or
176 the improvement of draft genome bins, as determined by Anvi'o real-time completion
177 and contamination scores.

178 Dereplication of the MAGs and selection of the representative MAG from the
179 dereplicated collections were conducted using the default settings for dRep (Olm et al.
180 2017). Default settings in dRep include dereplication of genomes with an average
181 nucleotide identity (ANI) of 0.95 and a minimum overlap of 10% between the two
182 genomes. dRep incorporates additional essential methods, including CheckM (Parks et
183 al. 2015) and FastANI (Jain et al. 2018). dRep uses completion and contamination
184 based on checkM, which were never at or above the 75% threshold for any of the
185 Patescibacteria. Patescibacteria MAGs were dereplicated separately without a checkM
186 quality score filter. We used the GTDB-Tk to assign taxonomy to each of the MAGs
187 recovered using default settings (Chaumeil et al. 2020)

188 To identify the phylogenomic relationships among the collection of dereplicated
189 MAGs, we first exported the amino acid sequence of the best hit for 71 single copy
190 genes (Bacteria_71). The amino acid sequences for these genes were aligned using
191 MUSCLE and the alignment was trimmed using trimAL v1.4 (Capella-Gutiérrez, Silla-
192 Martínez, and Gabaldón 2009). We reconstructed the phylogenetic tree according to the
193 WAG general matrix to model amino-acid exchange rate (Whelan and Goldman 2001)
194 using IQ TREE v2.2.6 (Minh et al. 2020). The fasta file of single copy gene sequences,
195 alignment, tree, and additional details of phylogenetic reconstruction are available in this
196 github repository https://github.com/jvineis/DEEP-CORE-MANUSCRIPT.git.
197 We mapped the metagenomic reads from each sample to the collection of
198 dereplicated MAGs using bowtie2 v2.5.3 (Langmead and Salzberg 2012). Unmapped
199 reads were filtered from the results and samtools v1.19.2 (Li et al. 2009) was used to
200 tabulate the number of reads recruited to each MAG. The relative abundance of each
201 MAG was estimated by dividing the number of reads mapped to the MAG by the
202 number of reads recruited to the non-redundant collection of MAGs.
203
204 **4. Identifying co-occurring MAGs using network reconstruction**
205 To identify groups of co-occurring genome populations that may be indicative of
206 a shared niche space and/or burial trajectory, we constructed a molecular ecological
207 network (MEN) using random matrix theory (RMT) according to the procedures
208 recommended by iNAP (Feng et al. 2022). RMT is more commonly used for functional
209 or phylogenetic marker genes but is broadly designed to identify co-occurrence patterns
210 among complex datasets that contain large numbers of variables (species occurrence,

211 microarray data, marker genes) (Gibson et al. 2013). The count matrix of reads
212 recruited to each of the 377 dereplicated MAG was used as the input for RMT MEN
213 construction. Following log transformation of the count matrix, an adjacency matrix was
214 calculated according to Pearson correlation coefficients. To separate significant co-
215 occurrence from noise, RMT estimates the nearest neighbor spacing distribution
216 (NNSD) within the entire correlation matrix. A random matrix of NNSD values will follow
217 a Gaussian distribution and a non-random matrix will follow a Poisson distribution (Luo
218 et al. 2007). To identify the threshold where the correlation estimates transition from
219 Gaussian to Poisson, we ran iterations of successively smaller correlations starting at 1
220 with a step size of 0.01. A Chi-square test was used to evaluate transition from a
221 Poisson to a Gaussian distribution at each step and iNAP created a plot of resulting p-
222 values to evaluate each step. Visual inspection of the cutoff indicated that correlations
223 below 0.92 were more likely due to random noise (Fig. S1). All correlations below this
224 0.92 cutoff were set to zero and a network was constructed. RMT network properties
225 were calculated for the resulting filtered network, including R-square of the power-law
226 relationship. A network containing few MAGs with large numbers of connections with
227 other MAGs will have connectivity that follows a power-law distribution. If the
228 connectivity doesn't fit the power-law distribution, this indicates that there are many
229 MAGs with high connectivity to other MAGs (a very dense network). Module separation
230 and identification of module hubs were calculated according to a greedy modularity
231 optimization (Newman 2004). Within-module (Z) and among-module connectivity (P)
232 were used to classify each MAG as a network hub ($Z > 2.5$ and $P > 0.62$), module hub
233 ($Z > 2.5$ and $P < 0.62$), connector ($Z <$ and $P > 0.62$), or peripheral ($Z < 2.5$ and $P <$

234 0.62) (Deng et al. 2012). Based on previous ecological interpretation of networks, the
235 peripheral, connector hub, module hub, and network hub might represent a continuum
236 from specialist to generalist in that order (Olesen et al. 2006). For our purposes of
237 identifying co-occurring genomes, we focused on the identification of modules, which
238 are interlinked subsets of MAGs, and connector hubs that could be important to the
239 stability of the different modules (Olesen et al. 2006).
240

241 **5. Metabolic potential and distribution of MAGs within identified network**
242 **modules.**

243 To estimate the differences in functional potential among the RMT modules, we
244 constructed a matrix composed of KEGG functional IDs obtained using anvi-estimate-
245 metabolism. MAGs that were included in modules containing fewer than four members
246 or not assigned to a module were also removed from the matrix. We constructed an
247 Atchinson distance matrix and built an NMDS ordination using the vegdist and
248 metaMDS functions respectively. We tested the influence of RMT module and
249 taxonomic classification at the phylum level on the community turnover using the envfit
250 function. All diversity analysis was conducted in R (R Foundation for Statistical
251 Computing 2021) with functions contained in the vegan package (Oksanen et al. 2024).
252 Relative abundance of MAGs within each module were visually inspected to identify
253 their distribution within the vertical sediment profile.
254

255 **6. Connector hub (Bathyarchaeia BA1) subnetwork genome scale metabolic**
256 **networks**

257 Visualization of the complete RMT network (described above) using Cytoscape
258 (Shannon et al. 2003) led to the identification of four modules with similar taxonomy,
259 functional profiles, and high relative abundance within deeper sediment layers. The
260 connector hub that was common across all four modules, Bathyarchaeia BA1, was used
261 to identify a subnetwork of MAGs that were positively connected and therefore
262 contained the potential for metabolic complementarity. Focusing on MAGs in this
263 subnetwork, we estimated the metabolic potential for key pathways related to
264 decomposition of organic compounds, aromatics, acetate, hydrogenases, and other
265 pathways important to carbon cycling within low energy sediment environments using
266 METABOLIC according to the default parameters (Zhou et al. 2022). We reconstructed
267 genome-scale metabolic networks (GSMNs) using gapseq (Zimmermann, Kaleta, and
268 Waschina 2021) and miscoto (Frioux et al. 2020) was employed to screen GSMNs for
269 key members of minimal communities required to produce the metabolites of the entire
270 community. Analysis of GSMNs was employed using Metag2Metabo (M2M) (Belcour et
271 al. 2020). This approach identifies putative metabolites produced by the co-occurring
272 members of the network module, the key microbial taxa required to produce these
273 metabolites, and interchangeable (redundant) members of the network module.
274

275 ## Results

276 **1. Diverse MAG populations were broadly distributed within salt marsh**
277 **sedimentary layers and both sites**

278 We generated 645.9 Gbp sequences from 55 samples collected within ~250 cm
279 of salt marsh sediment from six cores (Fig. 1). The manual genome binning and

280 refinement effort for each of the 55 samples recovered a total of 2,346 MAGs.
281 Dereplication resulted in a collection of 377 MAGs that were an average of 87%
282 complete and 2.7% redundant. The number of MAGs contained in each dereplicated
283 cluster ranged from 1 to 30 (Fig. 2). Some examples of genome populations
284 represented by a large cluster of dereplicated genomes include 25 independently
285 reconstructed *Ca. Aminicenans* that were reduced to two unique MAGs, 63
286 Actinobacteriota reduced to 4 MAGs, 52 *Bipolaricaulia* reduced to 6 MAGs, 85 WOR3-B
287 reduced to 11 MAGs, and 24 TA06 reduced to 1 unique MAG (Fig. 2). Many of the
288 MAGs were recovered independently from more than one depth and often from different
289 cores at locations adjacent to different creeks (Fig. 2). In some instances, MAGs from
290 the same dereplicated cluster were independently reconstructed from the top 10-20 cm
291 and below 200 cm. For example, a dereplicated WOR3 MAG contained nearly 30
292 independently assembled MAGs from samples that spanned the entire 10-240cm
293 vertical profile (Fig. 2). The Desulfobacterota, Bacteroidota, Actinobacteriota,
294 Planctomycetota, and Chloroflexota each contained several MAGs that were recovered
295 from all depths. Sparsely detected Proteobacteria, Gemmatimonadota, and
296 Asgardarchaeota were recovered predominantly from shallow sediment layers, 90cm
297 and above (Fig. 2).
298 The proportion of metagenomic sequences recruited (mapped) to our collection
299 of nonredundant MAGs was generally greater in sediment samples collected below 40
300 cm (Fig. S2). Read recruitment below 40 cm was at least 35% and reached nearly 60%
301 in most of the samples below 90 cm. Conversely, metagenomic sequences from

sediment samples collected from above 20 cm recruited less than 20% of sequences per sample (Fig. S2) and the number of MAGs recovered was generally lower.

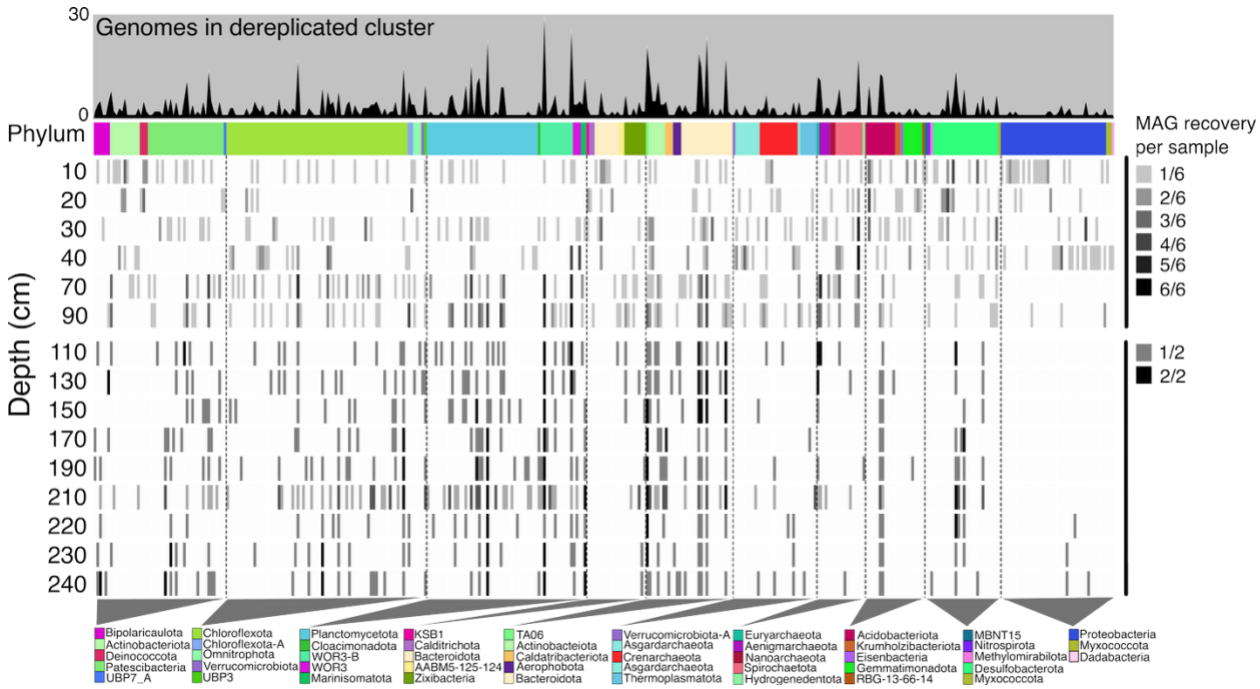

Figure 2. Summary of redundant genome recovery per sample. The line plot at the top of the figure (dark gray and black) shows how many genomes were grouped into the dereplicated genome cluster. The second layer from the top represents the phylum level classification for the representative MAG in the cluster. The heat map layers show the proportion of samples where a MAG in the dereplicated genome cluster was recovered. The key indicating how many of the same MAGs (identified by dRep) were collected per depth is shown on the right. The MAGs are organized according to the phylogenetic reconstruction outlined in the methods section. The phylum color key is shown at the bottom of the figure and the gray triangles above the phylum color align with the heatmap.

317

318 **2. Co-occurring MAGs**

319 *2.1 Strong positive correlations exist among groups of functionally similar MAGs in the*

320 *deeper sediment layers*

321 Based on MAG relative abundance, we identified a connected network containing

322 1547 positive connections (edges) among 226 of the 377 MAGs and zero negative

323 edges. Most of MAGs were peripheral nodes in the network, but one MAG

324 (Dehalococcoidales – UBA5760) was identified as a module hub and 15 MAGs were

325 classified as connector hubs (Fig. S3). Among the connector hubs were two

326 Bathyarchaeia classified as BA1, two Dehalococcoidales, Desulfatiglandales, and GIF9

327 MAGs. The R^2 of the power-law was 0.97, indicating a scale-free network where most

328 MAGs in the network have few connections. We chose to focus our functional

329 analysis on the top seven modules identified in the network because the remaining 11

330 modules contained fewer than 5 MAGs (Table S1).

331 Modules 1 and 2 contained the largest number of MAGs with a high degree of

332 connectivity within and between the two modules (Fig. 3A). Modules 1 and 2 were also

333 diverse, containing MAGs from 14 and 23 phyla respectively. MAGs within module 7

334 contained many positive links with modules 1 and 2 and the functional potential among

335 MAGs within these three linked modules was very similar (Fig. 3B, Fig. S4). However,

336 modules 1 and 2 contained larger dispersion in the ordination than module 7 due to the

337 presence of Patescibacteria, which were functionally distinct from other MAGs, largely

338 due to their limited functional potential (Fig 3B). Most of the Patescibacteria contained

339 fewer than 800 genes (Table S1). A relatively large proportion of MAGs in modules 1, 2,

340 and 7 (> 25%) contained pathways for complex carbon decomposition, fermentation,
341 amino acid metabolism, and several C1 pathways (Fig. S4). However, pathways for
342 carbon fixation, nitrogen and sulfur reduction, oxygen metabolism, and oxidative
343 phosphorylation were identified in a relatively lower proportion (Fig. S4). Connectivity
344 among modules 4 and 5 was sparse in comparison to the large number of positive
345 connections among modules 1, 2, and 7. However, the overall functional potential was
346 similar among all five modules (Fig. 3B).
347 Modules 3 and 6 contained relatively few members (Fig. 3A). However, the
348 potential for nitrogen and sulfur reduction, oxygen metabolism, carbon fixation, and
349 oxidative phosphorylation was generally higher than modules 1, 2, 4, 5, and 7 (Fig. S4).
350

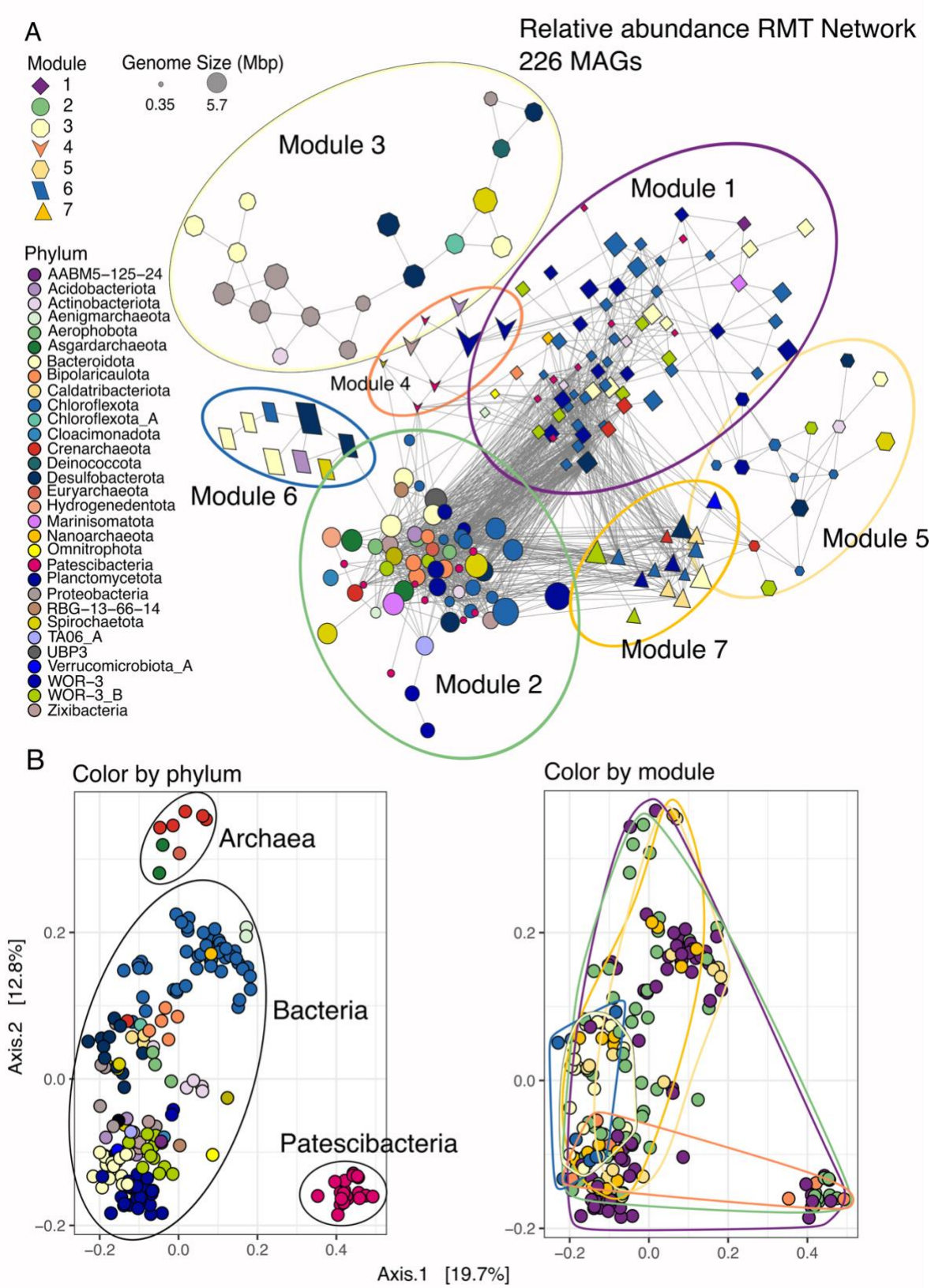
A
Relative abundance RMT Network
226 MAGs
Module
1
2
3
4
5
6
7
Genome Size (Mbp)
0.35
5.7
Phylum
AABM5−125−24
Acidobacteriota
Actinobacteriota
Aenigmarchaeota
Aerophobota
Asgardarchaeota
Bacteroidota
Bipolaricaulota
Caldatribacteriota
Chloroflexota
Chloroflexota_A
Cloacimonadota
Crenarchaeota
Deinococcota
Desulfobacterota
Euryarchaeota
Hydrogenedentota
Marinisomatota
Nanoarchaeota
Omnitrophota
Patescibacteria
Planctomycetota
Proteobacteria
RBG−13−66−14
Spirochaetota
TA06_A
UBP3
Verrucomicrobiota_A
WOR−3
WOR−3_B
Zixibacteria
Module 3
Module 1
Module 4
Module 6
Module 5
Module 7
Module 2
B
Color by phylum
Color by module
Archaea
Bacteria
Patescibacteria
Axis.2 [12.8%]
Axis.1 [19.7%]
0.2
0.0
−0.2
−0.2
0.0
0.2
0.4

351

352 Figure 3. A.) The random matrix theory derived co-occurrence network, based on MAG
353 relative abundance. The point size (genome size), color (phylum), and shape (module)
354 are used to describe each MAG in the network. All connections are significant and
355 positive. Ellipses are used to clarify the modules. B) The NMDS ordination of MAGs
356 included in the network based on KEGG functional potential. Both panels show the
357 same ordination, with the left panel colors indicating the phylum classification and right,
358 the module assignment. The key adjacent to panel A applies to the colors used for taxa
359 and modules shown in panel B.
360
361 *2.2 Modules containing widespread and abundant MAGs in sediment layers.*
362 The relative abundance of MAGs at the phylum level within a module was
363 consistent across sediment layers (Fig. 4). For example, the top four most abundant
364 phyla in module 1 included Chloroflexota, Planctomycetota, Bacteroidota, and
365 Actinobacteriota. In module 2, the cumulative relative abundance of Choloroflexota,
366 Planctomycetota, TA06, and WOR3-B were also among the most abundant phyla within
367 this module and were found in similar relative proportions in the sediment layers.
368 Despite the diversity of MAGs assigned to a particular phylum within a module, a
369 small number of MAGs were often the most abundant at all sediment depths. For
370 example, 12 of the 70 MAGs in module 1 represented the majority of reads recruited
371 (Fig. S5). The abundant MAGs in the module were distributed across 6 of the 13 phyla
372 in the module. Within module 1, 5 Chloroflexota MAGs were among the most abundant
373 (Fig. S5). Other phyla within the module were low diversity, such as TA06 in module 2,
374 where a single MAG was the sole contributor to the phylum level abundance patterns.

375 Although often detected in the entire depth profile, MAGs within modules 1, 2 and
376 7 were especially abundant below 20 cm (Fig. 4). Modules 1 and 2 contained several
377 Chloroflexota MAGs that collectively recruited at least 15% of the mapped reads.
378 Average coverage of these MAGs was over 50X in the majority of samples below 40
379 cm. Module 2 contained two of the most abundant MAGs below 40 cm, TA06 and
380 Bipolaricaulota, which recruited nearly 15% of mapped reads in many samples below
381 100 cm. The peak relative abundance of MAGs in modules 1, 2, 5, and 7 were distinct,
382 with module 1 peaking in abundance at 70-110 cm, module 2 peaking in all samples
383 below 100 cm, module 5 peaking at 30 - 40 cm, and module 7 peaking at 150 – 250 cm
384 (Fig 4).

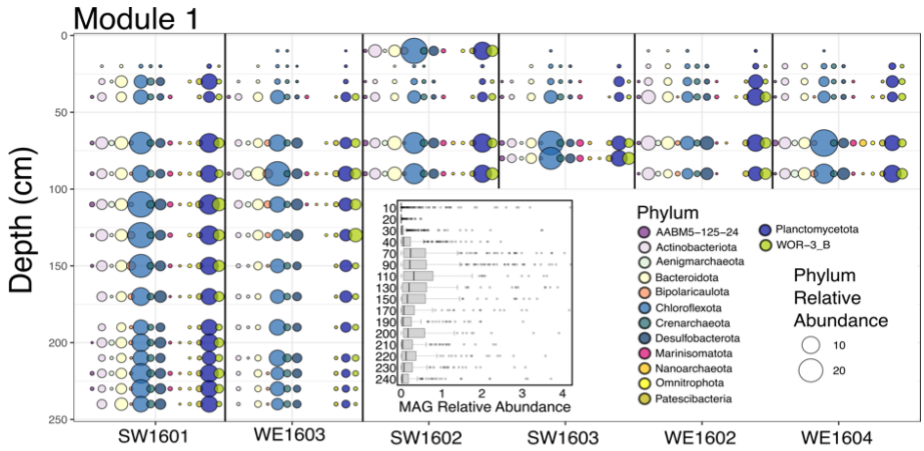
Module 1
Depth (cm)
SW1601
WE1603
SW1602
SW1603
WE1602
WE1604
MAG Relative Abundance
Phylum
AABM5-125-24
Actinobacteriota
Aenigmarchaeota
Bacteroidota
Bipolaricaulota
Chloroflexota
Crenarchaeota
Desulfobacterota
Marinisomatota
Nanoarchaeota
Omnitrophota
Patescibacteria
Planctomycetota
WOR-3_B
Phylum Relative Abundance

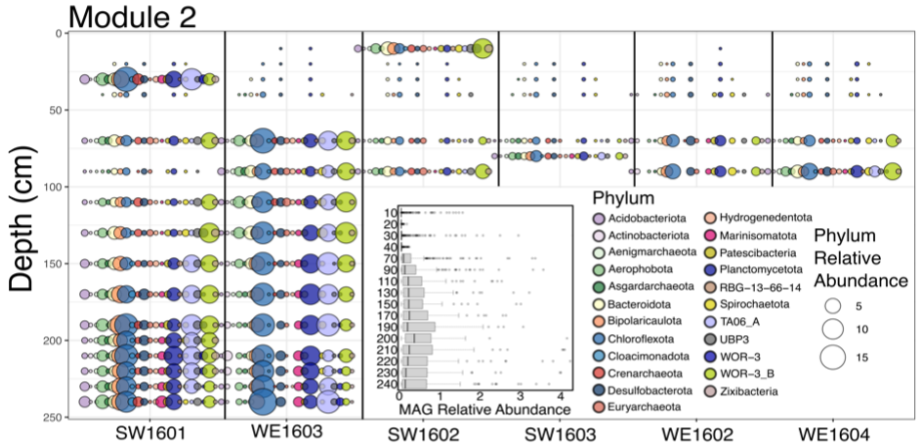
Module 2
Depth (cm)
SW1601
WE1603
SW1602
SW1603
WE1602
WE1604
MAG Relative Abundance
Phylum
Acidobacteriota
Actinobacteriota
Aenigmarchaeota
Aerophobota
Asgardarchaeota
Bacteroidota
Bipolaricaulota
Chloroflexota
Cloacimonadota
Crenarchaeota
Desulfobacterota
Euryarchaeota
Hydrogenedentota
Marinisomatota
Patescibacteria
Planctomycetota
RBG-13-66-14
Spirochaetota
TA06_A
UBP3
WOR-3
WOR-3_B
Zixibacteria
Phylum Relative Abundance

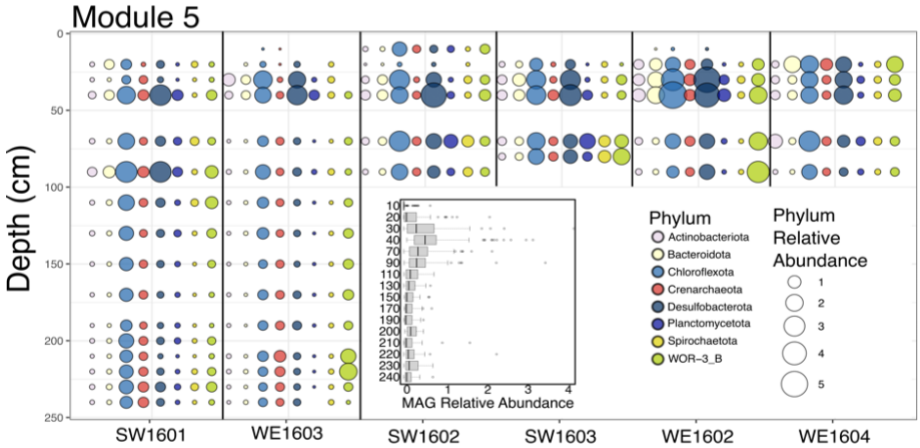
Module 5
Depth (cm)
SW1601
WE1603
SW1602
SW1603
WE1602
WE1604
MAG Relative Abundance
Phylum
Actinobacteriota
Bacteroidota
Chloroflexota
Crenarchaeota
Desulfobacterota
Planctomycetota
Spirochaetota
WOR-3_B
Phylum Relative Abundance

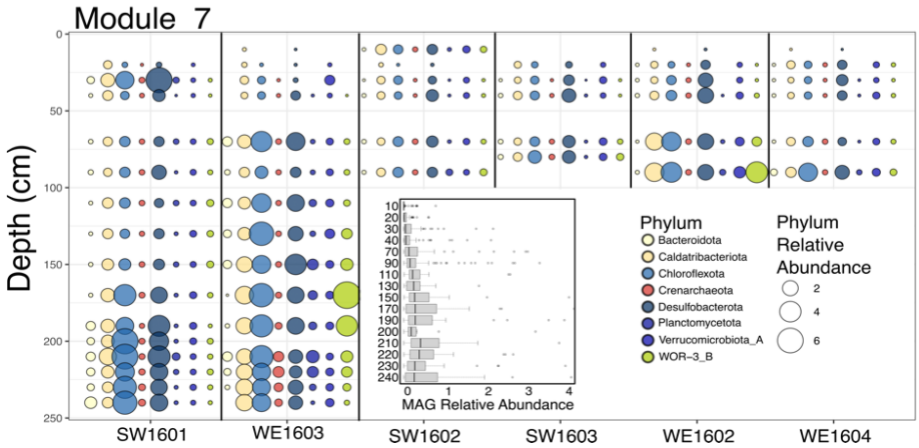
Module 7
Depth (cm)
SW1601
WE1603
SW1602
SW1603
WE1602
WE1604
MAG Relative Abundance
Phylum
Bacteroidota
Caldatribacteriota
Chloroflexota
Crenarchaeota
Desulfobacterota
Planctomycetota
Verrucomicrobiota_A
WOR-3_B
Phylum Relative Abundance

386 Figure 4. Bubble plots for the cumulative phylum level relative abundance of MAGs
387 contained in each of the network modules. Relative abundance (size of the bubble)
388 indicates the percentage of reads mapped to the MAGs glommed at the phylum level
389 relative to the number of reads mapped to the sample. The colors for each phylum are
390 congruent across all four panels. The box-whisker relative abundance plots nested
391 within each box describe the relative abundance of MAGs in the module at each depth.
392

393 *3.3 Unconnected MAGs are dominant in the upper 40 cm and potentially have a niche*
394 *in the deepest sediment*

395 In addition to MAGs that were associated with the modules described above,
396 there were numerous unconnected MAGs that were predominantly located in sediments
397 at or above 40 cm (Fig. S4). Proteobacteria (Pseudolabrys and Methyloceanibacter)
398 and Crenarchaeota (Nitrososphaeraceae and Bathyarchaeia BA1) MAGs were among
399 the most abundant unconnected MAGs. However, we also observed MAGs within many
400 sediment layers that were abundant both in the upper 40 cm and below 200 cm within
401 the core collected from West creek (WE3) (Fig. S6). Although they maintained a patchy
402 distribution in the surface, the relative abundance was consistent at 200-240 cm (Fig.
403 S6). *Methyloceanibacter* MAGs identified in this “bimodal” group are putative bacterial
404 methylotrophs (Vekeman et al. 2016), but none of the mags contained the methane
405 monooxygenase or co-methyltransferase genes. Bimodal Nitrososphaeraceae MAGs
406 contained ammonia oxidation potential (*amo*) and the *Pseudolabrys* contained sulfur
407 oxidation (*sox*), sulfur reduction (*dsr, apr, sat*), and nitrate reduction potential (*narG*)

408 (Fig. S6). These functions suggest a mix of aerobic and anaerobic potential within the
409 deepest layers sampled in the West creek sediment core.
410
411 *3.4 Bathyarchaeia BA1 are potentially important facilitators of abundant deep sediment*
412 *communities*
413 Because of the potentially important ecological role of Bathyarchaeia BA1 MAGs
414 in the network as connector hubs (Fig. S3) and global significance of this family to
415 carbon cycling (Hou et al. 2023), we focused on these MAGs and the connections to
416 other MAGs in the network to understand the potential relevance to carbon cycling. Our
417 network analysis identified 2 separate Bathyarchaeia BA1 MAGs that were connector
418 hubs in the RMT network (Fig. S3). To explore the potential role of these Bathyarchaeia
419 BA1 we created a subnetwork of MAGs that are directly connected to the Bathyarchaeia
420 MAGs, resulting in a total of 33 MAGs in the subnetwork (Fig 5A). Among the 12
421 different orders contained in the subnetwork were members of Bipolaricaulia, GIF9,
422 WOR3, Desulfatiglandales, and Caldatribacteriota and each of the four modules (1, 2, 5,
423 and 7) were represented (Fig. 5A). The relative abundance of members at the phylum
424 level in this subnetwork was also consistent across many of the samples (Fig. 5B).
425
426 **4. Putative functional complementarity among Bathyarchaeia subnetwork MAGs**
427 **suggests potential decomposition of hydrocarbon and aromatics**
428 *4.1 Consistent relative abundance among members of the Bathyarchaeia subnetwork*
429 Within the Bathyarchaeia subnetwork, GIF9 MAGs were the most abundant,
430 totaling 8 MAGs, all of which are putative acetogens based on their functional profile.

431 Six GIF9 MAGs were located in the same module (module 2), indicating a close
432 ecological connection and yet they were not identified as functionally redundant
433 members of the community according to the M2M analysis. The collective GIF9 MAG
434 relative abundance reached 15% in many of the samples below 20 cm, but like all
435 MAGs in the subnetwork, they were not excluded from the upper 20 cm (Fig. 5B).
436 Desulfatiglandales, Dehalococcoidales, and Planctomycetota were also among the
437 most abundant MAGs in the subnetwork and occurred at similar cumulative relative
438 abundances. The high correlation among these MAGs detected in the network is
439 reflected in the consistent relative abundance of the group members within a core and
440 generally across all six cores (Fig. 5B).
441
442 *4.2 Bathyarchaeia BA1 subnetwork MAGs use cooperative metabolism to degrade*
443 *aromatics*
444 M2M identified the putative functions of each community member and the added
445 value metabolites produced by minimal communities. An added value metabolite is one
446 produced through complimentary metabolism among the microbes in a minimal
447 community, and a minimal community is defined as a cohort of MAGs required to
448 produce the entire set of metabolites in the collection of genomes. We found 82
449 metabolites that were producible by each of the 33 MAGs in the subnetwork (core
450 functions) and 1098 total metabolites could be produced by the individual organisms all
451 together (collective functions). The added value of cooperation within the minimal
452 communities required 22 bacteria and 20 essential symbionts to produce an additional
453 228 compounds. These 228 compounds were only possible when all members of a

454 minimal community had the potential to exchange metabolites. Redundant members of
455 the community that were identified in at least one, but not all minimal communities
456 included Dehalococcoidia – RBG-16-60-22, Caldatribacteriota JS1, Dehalococcoidia
457 AB-539-J10, and Dehalococcoidia UBA5760.

458 Among the 228 compounds that could be formed solely if organisms exchanged
459 compounds, key metabolites involved in anaerobic decomposition of aromatic
460 compounds were identified and the presence of the genes conferring capacity for these
461 putative functions were confirmed by METABOLIC. Benzoyl-CoA reductase (*bcr*) was
462 identified in the genomes of three Desulfatiglandales, a novel order of Cloroflexota, and
463 Bathyarchaeia. Genes to produce benzoyl-CoA from phenol (*ubiX*/*bsdC*) occurred in
464 two of the Desulfatiflandales, the Bathyarchaeia and Bacteroidales MAGs (Fig. 5C).
465 Phenylacetyl-CoA was also identified as a metabolite putatively produced through
466 functional complementarity within the subnetwork.

467

468 *4.3 Genomic potential for acetogenesis and metabolic versatility is common among the*
469 *Bathyarchaeia BA1 subnetwork*

470 Genes for heterotrophic and autotrophic acetogenesis, primarily through the
471 Wood-Ljungdahl (WL) pathway, were detected in 25 of the 33 genomes in the
472 Bathyarchaeia B26-1 subnetwork (Fig. 5C). These genes included acetyl-CoA
473 dehydrogenase (*acdA*), acetate kinase (*ack*), and phosphate acetyltransferase (*pta*).
474 *acdA* was the most commonly detected gene indicating acetogenic metabolism, and *acs*
475 (Acetyl-CoA synthetase) was commonly detected within the same MAG (Table S2). The
476 co-occurrence of genes encoding a putative WL pathway within most genomes and a

477 formate oxidation gene (*fae*) required to convert CO_2 into formate provides additional
478 evidence for synthesis of acetate from H_2 and CO_2. The genomic potential for the
479 production of acetate enabled by carbon fixation via the WL pathway was observed in
480 Desulfatiglandales, Bathyarchaeia, Dehalococcoidales, Chloroflexota, GIF9,
481 Bipolaricaulia, and Planctomycetota MAGs in the subnetwork (Fig. 5C). A WL pathway
482 was not detected in Caldatribacteriota, WOR3, and Bacteroidales. Instead, these MAGs
483 might produce acetate through fermentation of pyruvate or lactate. Most acetogens in
484 the network contain genes indicative of a flexible metabolic capacity through autotrophic
485 and/or fermentative acetate production (Fig. 5C).
486 We detected several additional pathways potentially related to energy
487 conservation among the members of the subnetwork. The presence of methane
488 monooxygenase regulatory protein (*mmoBD*) in Bipolaricaulia and Desulfatiglandales
489 (Fig. 5C) suggests methane oxidation potential. Additionally, aerobic carbon monoxide
490 dehydrogenase *coxSM* was detected in members of Bipolaricaulia, Caldatribacteriota,
491 Bathyarchaeia TCS64, and Desulfatiglandales. Additional pathways include selenate or
492 arsenate reduction potential in most of the subnetwork MAGs and one of the GIF9
493 MAGs contained genes for both pathways.
494
495

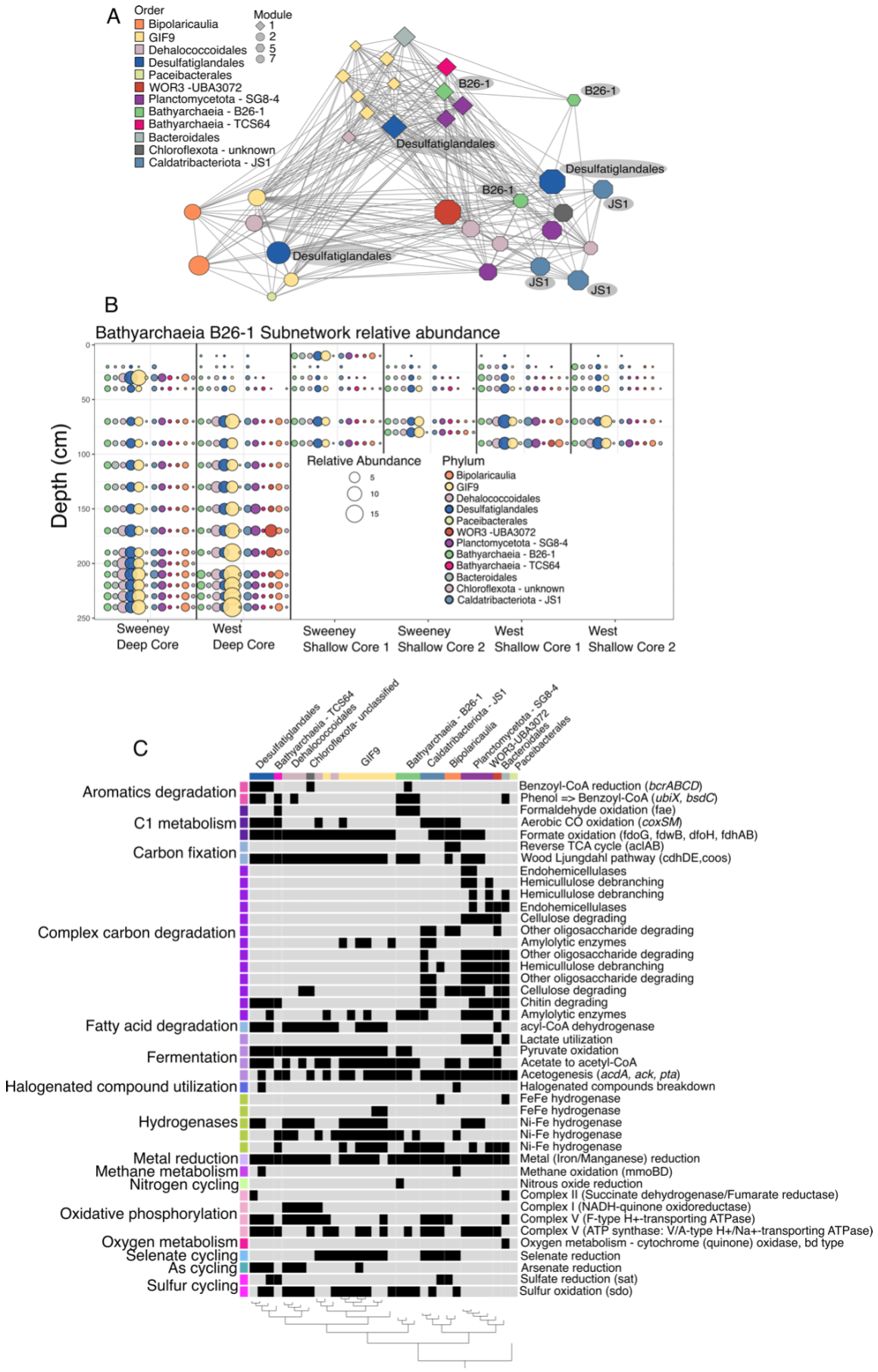
A
Order
Bipolaricaulia
GIF9
Dehalococcoidales
Desulfatiglandales
Paceibacterales
WOR3 -UBA3072
Planctomycetota - SG8-4
Bathyarchaeia - B26-1
Bathyarchaeia - TCS64
Bacteroidales
Chloroflexota - unknown
Caldatribacteriota - JS1
Module
1
2
5
7
B26-1
B26-1
Desulfatiglandales
Desulfatiglandales
B26-1
JS1
Desulfatiglandales
JS1
JS1
B
Bathyarchaeia B26-1 Subnetwork relative abundance
Depth (cm)
0
50
100
150
200
250
Relative Abundance
5
10
15
Phylum
Bipolaricaulia
GIF9
Dehalococcoidales
Desulfatiglandales
Paceibacterales
WOR3 -UBA3072
Planctomycetota - SG8-4
Bathyarchaeia - B26-1
Bathyarchaeia - TCS64
Bacteroidales
Chloroflexota - unknown
Caldatribacteriota - JS1
Sweeney Deep Core
West Deep Core
Sweeney Shallow Core 1
Sweeney Shallow Core 2
West Shallow Core 1
West Shallow Core 2
C
Desulfatiglandales
Bathyarchaeia - TCS64
Dehalococcoidales
Chloroflexota- unclassified
GIF9
Bathyarchaeia - B26-1
Caldatribacteriota - JS1
Bipolaricaulia
Planctomycetota - SG8-4
WOR3-UBA3072
Bacteroidales
Paceibacterales
Aromatics degradation
C1 metabolism
Carbon fixation
Complex carbon degradation
Fatty acid degradation
Fermentation
Halogenated compound utilization
Hydrogenases
Metal reduction
Methane metabolism
Nitrogen cycling
Oxidative phosphorylation
Oxygen metabolism
Selenate cycling
As cycling
Sulfur cycling
Benzoyl-CoA reduction (bcrABCD)
Phenol => Benzoyl-CoA (ubiX, bsdC)
Formaldehyde oxidation (fae)
Aerobic CO oxidation (coxSM)
Formate oxidation (fdoG, fdwB, dfoH, fdhAB)
Reverse TCA cycle (aclAB)
Wood Ljungdahl pathway (cdhDE,coos)
Endohemicellulases
Hemicullulose debranching
Hemicullulose debranching
Endohemicellulases
Cellulose degrading
Other oligosaccharide degrading
Amylolytic enzymes
Other oligosaccharide degrading
Hemicullulose debranching
Other oligosaccharide degrading
Cellulose degrading
Chitin degrading
Amylolytic enzymes
acyl-CoA dehydrogenase
Lactate utilization
Pyruvate oxidation
Acetate to acetyl-CoA
Acetogenesis (acdA, ack, pta)
Halogenated compounds breakdown
FeFe hydrogenase
FeFe hydrogenase
Ni-Fe hydrogenase
Ni-Fe hydrogenase
Ni-Fe hydrogenase
Metal (Iron/Manganese) reduction
Methane oxidation (mmoBD)
Nitrous oxide reduction
Complex II (Succinate dehydrogenase/Fumarate reductase)
Complex I (NADH-quinone oxidoreductase)
Complex V (F-type H+-transporting ATPase)
Complex V (ATP synthase: V/A-type H+/Na+-transporting ATPase)
Oxygen metabolism - cytochrome (quinone) oxidase, bd type
Selenate reduction
Arsenate reduction
Sulfate reduction (sat)
Sulfur oxidation (sdo)

Figure 5. A) The submodule of tightly correlated MAGs with connectivity among the four subsurface modules. The shape in the network indicates module origin of each MAG, the size represents the number of genes in the MAG, and the color is used for taxonomic classification. Gray lines connecting the MAGs represent significant positive correlations. B.) Bubble plot of relative abundance for MAG phylum level relative abundance within the vertical profile of the sediment. The color of the bubble is based on the phylum classification and matches the color in panel A. C) Select functional annotation for all MAGs in the network. Functional potential of each MAG in the network is described as presence (black bar) or absence (gray bar) for each function. Major functional categories are shown on the left of the panel and the taxonomic classification of each MAG is shown at the top. MAGs are organized according to presence-absence of the genes in the display and the hierarchical clustering tree is displayed at the bottom of the panel.

Discussion

Salt marsh sediments contain diverse microbial communities with vast numbers of uncultivated microbial organisms that are important to carbon storage and biogeochemical cycling. Within the complex microbial communities inhabiting these sediments, we identified metabolic complementarity important to cycling pools of aromatic carbon among co-occurring groups of microbes. Bathyarchaeia BA1 was a key member of each group of MAGs that were uniquely distributed within the sediment profile, although they were primarily located below the influence of the dynamic upper layers of the sediment. Another key finding was that similar populations exist throughout

520 the entire depth profile of multiple cores that spans nearly 3000 years of sediment
521 accumulation (Bulseco-McKim 2018). This pattern may be the result of a burial process
522 followed by environmental selection and slow growth rates. Conversely, the upper
523 layers of sediment contain diverse MAGs with greater functional potential representing
524 the canonical pathways commonly associated with salt marsh microbial communities
525 (Baker et al. 2015a; Tobias and Neubauer 2018). Our results are important for
526 understanding how the pools of organic carbon are shaped by microbial communities
527 within the less well characterized subsurface because we identify which microbes are
528 co-located, what forms of carbon may be made accessible due to metabolic
529 complementarity, and the underlying biogeochemical processes that preserve these
530 relationships.
531
532 **1. Metabolic flexibility is a key feature among MAGs in the zone of plant and tidal**
533 **influence.**
534 Plant roots and rhizomes along with bioturbating organism and other structural
535 features can increase permeability in the upper layers of the sediment (Guimond et al.
536 2020; Moffett et al. 2012; Xiao et al. 2019) and these dynamic conditions potentially
537 lead to observed high diversity of microbial communities in the upper sediment layers.
538 Redox conditions and carbon availability can change rapidly in the upper sediment
539 layers, creating conditions where metabolic flexibility would be favored. As a result,
540 there is a decreased need for metabolic handoffs among members of the community.
541 Most of the MAGs that were unconnected in our network analysis were localized
542 in the dynamic upper layers of the sediment and did not occur below 90 cm. The

543 unconnected MAGs contained striking genomic versatility including the capacity to
544 utilize multiple electron acceptors for oxidation of diverse carbon sources, conduct
545 fermentation, and fix inorganic carbon. Many of the unconnected Proteobacteria and
546 Desulfobacterota MAGs contain the genomic potential for each of these metabolic
547 pathways in a single organism which was observed previously in similar sediments
548 (Vineis et al. 2023). This metabolic flexibility allows each of the members of the
549 community to inhabit a variety of conditions and this strategy makes sense given the
550 dynamic nature of these sediments. Members of these communities contain canonical
551 pathways that are commonly associated with carbon cycling in salt marsh sediments
552 including fermentation, denitrification, and sulfate reduction (Baker et al. 2015a).
553

554 **2. Organic carbon decomposition in deeper sediment layers is facilitated by co-**
555 **occurring community members with complimentary metabolic pathways**

556 The consistency in relative abundance among members within the core
557 Bathyarchaeia subnetwork is a potential result of metabolic handoffs. Of particular
558 significance is the detection of benzoyl-CoA as a metabolite that could only be produced
559 by Bathyarchaeia, Dehalococcoidia, and Desulfatiglandales through metabolic handoffs
560 in the community. Benzoyl-CoA is a known intermediate involved in the anaerobic
561 decomposition of aromatic compounds toluene, phenol, ethylbenzene and benzoate
562 (Carmona et al. 2009; Porter and Young 2014). Under anaerobic conditions, reduction
563 of benzoyl-CoA leads to the production of acetyl-CoA which can enter into central
564 metabolic pathways for growth and energy conservation (Porter and Young 2014).
565 Phenylacetyl-CoA was also putatively produced through metabolic complementarity and

566 is similar to benzoly-CoA, leading to the potential production acetyl-CoA/succinyl-CoA.
567 These metabolic pathways, central to aromatic decomposition are only possible due to
568 the potential metabolic handoffs among the subnetwork members. Although it is
569 possible that other combinations of MAGs could lead to the decomposition of aromatics,
570 co-occurrence provides additional support that handoffs among the genome populations
571 identified here are likely to occur in the environment.

572 Syntrophic interactions between a bacterial fermenter and CO_2 reduction are
573 often cited as important to the decomposition of aromatic carbon (Dai et al. 2024; Qiu et
574 al. 2006, 2008). The collective functional profile of the Bathyarchaeia subnetwork
575 suggests that the initial fermentation of complex organic carbon is conducted by
576 members of the Planctomycetota, WOR3, JS1 and others, followed by secondary
577 decomposition of aromatics by Bathyarchaeia, Deslufatiglandales, Chloroflexota. The
578 products of secondary fermentation, including H_2 and formate, usually used by
579 methanogens, are instead potentially being used by a diverse group of acetogens.
580 Acetogens grow on organic materials derived from cellulose, lignin, alcohols,
581 hemicellulose, and chitin within energy depleted sediments (Lever 2012; Yu et al. 2018),
582 and there is evidence for the use of lignin as an energy source in Bathyarchaeota (Yu et
583 al. 2018).

584 These results suggest a central mechanism for carbon cycling among closely
585 coupled consortia within the sediment layers of salt marsh sediment. While this process
586 may be very slow, we have evidence from amplicon analysis of cDNA, that these
587 communities are active (Bulseco-McKim 2018). Conversion of these aromatics into

588 microbial biomass suggests that there may be a relevant cycling and/or recycling of
589 carbon stabilized by microbial activity even within these energy depleted sediments.

590 **3. Burial as a mechanism for aggregating putative consortia**

591 Burial as a mechanism for co-occurrence patterns has been suggested in energy
592 starved deep marine sediments where selection on the microbial community is thought
593 to result in low diversity (Kirkpatrick et al. 2019; Nayfach et al. 2021; Walsh et al. 2016).
594 Previous studies of microbial turnover within salt marshes described seasonal and
595 transect community compositional changes (Tebbe et al. 2022; Yao et al. 2019) or
596 succession along a chronosequence (Dini-Andreote et al. 2014; Wang et al. 2017).
597 However, the composition and stability of microbial communities within salt marsh
598 sediments remains relatively uncharacterized at the depths examine here.

599 Our study of the vertical sediment profile recovered two pieces of evidence that
600 suggests burial is a likely mechanism for the distribution of closely associated consortia.
601 The first observed pattern suggestive of burial was the recovery of MAGs assembled
602 independently from multiple depths in the same core that were dereplicated into a single
603 genome population. One of the strongest examples of this was observed in the
604 candidate phylum TA06, where a single population was recovered from 24 of the 55
605 samples, including every depth fraction except 10 cm. For dereplication to occur at this
606 scale (> 95% identity among MAGs in the dereplicated cluster), genome populations
607 would have experienced limited evolution over the nearly 3000 yrs of separation that
608 exists between the surface and bottom of the core. The second observed pattern was
609 the consistent relative abundance of MAGs within each module, relative to each other at
610 the phylum level (Fig. 4). The consistent relative abundance patterns among MAGs

611 within a module was observed both within the vertical sampling of an individual core and
612 across multiple cores. This is not to say that the relative abundance of members within
613 a module are the same at every depth across all cores. However, when the MAGs were
614 identified in a sample, they generally appear in similar ratios. The ratios of microbial
615 taxa might reflect the proportions required to support syntrophic interactions.

616 Similar compositions of sediment communities in marine systems have been
617 recovered from geographically distant communities (although at high taxonomic levels)
618 and were presumed to be subseafloor specialists (Inagaki et al. 2006; Petro et al. 2017,
619 2019). However, our data suggest that the same populations were buried within the
620 sediment, essentially preserving the population through high selection coupled with slow
621 growth.

622 The low porosity, small particle size, and low circulation observed in salt marsh
623 sediments on the East Coast of the US (Guimond and Tamborski 2021) provide
624 additional support to co-occurrence shaped by burial that we observed in our genomic
625 data. The turnover of water within the sediment can require 30-90 years (Guimond and
626 Tamborski 2021), depending on the marsh system, indicating that water flow from
627 groundwater or surface sources may be limited. These physical characteristics present
628 significant barriers to the dispersal of subsurface communities, leaving burial as a likely
629 mechanism. One caveat to the low porosity and water flow are the observations in the
630 deepest sediment layers collected from West Creek where we observed members of
631 the community that require oxygen. We speculate that the groundwater may potentially
632 “well up” from below the bedrock or sand located beneath the salt marsh platform at this
633 site.

5. Conclusion

The metabolic connections identified among correlated members of the microbial community provide key insights into how carbon is cycled by microbial communities within salt marsh sediments. Additionally, these results provide evidence for the successional mechanisms important to understanding the assembly and distribution of these communities. Our analysis identifies syntrophy among members of a putative core consortia that provides a potential mechanistic understanding of organic matter decomposition. The process begins with decomposers of complex carbon, followed by aromatic decomposition, coupled with acetogenic energy conservation and finally oxidation of acetate through arsenate or selenate reduction. These findings represent a significant step forward in our understanding of how microbial communities survive within these energy limited systems and contribute to the stability of soil organic carbon in this blue carbon system. The persistent conversion of soil organic carbon by the microbial community indicates that the pools of carbon potentially originating from plant material undergo decomposition and transformation even under energy depleted conditions.

Data Availability

The data described here are described in the U.S. Department of Energy (DOE) Facilities Integrating Collaborations for User Science (FICUS) grant titled “Combining high resolution organic matter characterization and microbial meta-omics to assess the effects of nutrient loading on salt marsh carbon sequestration” (proposal ID = 503576,

657 https://genome.jgi.doe.gov/portal/Comhiguestration/Comhiguestration.info.html).

658 Supplemental data can be accessed using this link to a publicly available github page

659 https://github.com/jvineis/DEEP-CORE-MANUSCRIPT.git

660

661 Acknowledgements

662 Samples were collected from the Plum Island Ecosystems LTER, which is supported by

663 NSF (OCE 2224608) and from the NSF funded TIDE project (DEB 1902712).

664 Sequencing was conducted at the Joint Genome Institute through a funded Facilities

665 Integrating Collaborations for User Science (FICUS) grant (proposal ID 503576).

666 Additional funding for this project was provided by the Simons Foundation (Grant

667 #1247132 to ZGC, and Grant #01248016 to JLB), and the Department of Energy (DOE

668 DE-SC0024270). This publication is number XXX from the Marine Science Center.

669

670 **References**

671

672 Alneberg, Johannes, Brynjar Smári Bjarnason, Ino De Bruijn, Melanie Schirmer, Joshua Quick,
673 Umer Z. Ijaz, Leo Lahti, Nicholas J. Loman, Anders F. Andersson, and Christopher Quince.
674 2014. "Binning Metagenomic Contigs by Coverage and Composition." *Nature Methods*
675 11(11):1144–46. doi:10.1038/nmeth.3103.

676 Arndt, Sandra, B. B. Jørgensen, D. E. LaRowe, J. J. Middelburg, R. D. Pancost, and P. Regnier.
677 2013. "Quantifying the Degradation of Organic Matter in Marine Sediments: A Review and
678 Synthesis." *Earth-Science Reviews* 123:53–86. doi:10.1016/j.earscirev.2013.02.008.

679 Baker, Brett J., Cassandre Sara Lazar, Andreas P. Teske, and Gregory J. Dick. 2015a. "Genomic
680 Resolution of Linkages in Carbon, Nitrogen, and Sulfur Cycling among Widespread Estuary
681 Sediment Bacteria." *Microbiome* 3(1). doi:10.1186/s40168-015-0077-6.

682 Baker, Brett J., Cassandre Sara Lazar, Andreas P. Teske, and Gregory J. Dick. 2015b. "Genomic
683 Resolution of Linkages in Carbon, Nitrogen, and Sulfur Cycling among Widespread Estuary
684 Sediment Bacteria." *Microbiome* 3(1):1–12. doi:10.1186/s40168-015-0077-6.

685 Bankevich, Anton, Sergey Nurk, Dmitry Antipov, Alexey A. Gurevich, Mikhail Dvorkin, Alexander
686 S. Kulikov, Valery M. Lesin, Sergey I. Nikolenko, Son Pham, Andrey D. Prjibelski, Alexey V.
687 Pyshkin, Alexander V. Sirotkin, Nikolay Vyahhi, Glenn Tesler, Max A. Alekseyev, and Pavel
688 A. Pevzner. 2012. "SPAdes: A New Genome Assembly Algorithm and Its Applications to

Single-Cell Sequencing." *Journal of Computational Biology* 19(5):455–77. doi:10.1089/cmb.2012.0021.

Belcour, Arnaud, Clémence Frioux, Méziane Aite, Anthony Bretaudeau, Falk Hildebrand, and Anne Siegel. 2020. "Metage2Metabo, Microbiota-Scale Metabolic Complementarity for the Identification of Key Species." *ELife* 9. doi:10.7554/eLife.61968.

Boschker, H. T. S., J. F. C. De Brouwer, and T. E. Cappenberg. 1999. *The Contribution of Macrophyte-Derived Organic Matter to Microbial Biomass in Salt-Marsh Sediments: Stable Carbon Isotope Analysis of Microbial Biomarkers*. Vol. 44.

Bulseco, Ashley N., Anne E. Giblin, Jane Tucker, Anna E. Murphy, Jonathan Sanderman, Kenly Hiller-Bittrolff, and Jennifer L. Bowen. 2019. "Nitrate Addition Stimulates Microbial Decomposition of Organic Matter in Salt Marsh Sediments." *Global Change Biology* 25(10):3224–41. doi:10.1111/gcb.14726.

Bulseco, Ashley N., Joseph H. Vineis, Anna E. Murphy, Amanda C. Spivak, Anne E. Giblin, Jane Tucker, and Jennifer L. Bowen. 2020. "Metagenomics Coupled with Biogeochemical Rates Measurements Provide Evidence That Nitrate Addition Stimulates Respiration in Salt Marsh Sediments." *Limnology and Oceanography* 65(S1):S321–39. doi:10.1002/lno.11326.

Bulseco-McKim. 2018. "Nitrate as an Electron Acceptor in Microbial Decomposition of Salt Marsh Sediment Organic Matter and Implications for Carbon Storage." Northeastern University.

Bushnell, B. 2021. "BBMap." https://sourceforge.net/projects/bbmap/.

Campbell, Anthony D., Lola Fatoyinbo, Liza Goldberg, and David Lagomasino. 2022. "Global Hotspots of Salt Marsh Change and Carbon Emissions." *Nature* 612(7941):701–6. doi:10.1038/s41586-022-05355-z.

Capella-Gutiérrez, Salvador, José M. Silla-Martínez, and Toni Gabaldón. 2009. "TrimAl: A Tool for Automated Alignment Trimming in Large-Scale Phylogenetic Analyses." *Bioinformatics* 25(15):1972–73. doi:10.1093/bioinformatics/btp348.

Carmona, Manuel, María Teresa Zamarro, Blas Blázquez, Gonzalo Durante-Rodríguez, Javier F. Juárez, J. Andrés Valderrama, María J. L. Barragán, José Luis García, and Eduardo Díaz. 2009. "Anaerobic Catabolism of Aromatic Compounds: A Genetic and Genomic View." *Microbiology and Molecular Biology Reviews* 73(1):71–133. doi:10.1128/MMBR.00021-08.

Chaumeil, Pierre Alain, Aaron J. Mussig, Philip Hugenholtz, and Donovan H. Parks. 2020. "GTDB-Tk: A Toolkit to Classify Genomes with the Genome Taxonomy Database." *Bioinformatics* 36(6):1925–27. doi:10.1093/bioinformatics/btz848.

Dai, Shixiang, Falk Harnisch, Micjel Chávez Morejón, Nina Sophie Keller, Benjamin Korth, and Carsten Vogt. 2024. "Microbial Electricity-Driven Anaerobic Phenol Degradation in Bioelectrochemical Systems." *Environmental Science and Ecotechnology* 17:100307. doi:10.1016/j.ese.2023.100307.

Deng, Ye, Yi-Huei Jiang, Yunfeng Yang, Zhili He, Feng Luo, and Jizhong Zhou. 2012. "Molecular Ecological Network Analyses." *BMC Bioinformatics* 13(1):113. doi:10.1186/1471-2105-13-113.

Dini-Andreote, Francisco, Michele de Cássia Pereira e Silva, Xavier Triadó-Margarit, Emilio O. Casamayor, Jan Dirk van Elsas, and Joana Falcão Salles. 2014. "Dynamics of Bacterial Community Succession in a Salt Marsh Chronosequence: Evidences for Temporal Niche Partitioning." *The ISME Journal* 8(10):1989–2001. doi:10.1038/ismej.2014.54.

Erb, Hailey, Ashley Keiser, and Kristen M. DeAngelis. 2024. “Salt Marsh Soil Organic Carbon Is Regulated by Drivers of Microbial Activity.” *Sustainable Microbiology* 1(1). doi:10.1093/sumbio/qvae009.

Eren, A. Murat, Özcan C. Esen, Christopher Quince, Joseph H. Vineis, Hilary G. Morrison, Mitchell L. Sogin, and Tom O. Delmont. 2015. “Anvi’o: An Advanced Analysis and Visualization Platform for ‘omics Data.” *PeerJ* 3:e1319. doi:10.7717/peerj.1319.

Eren, A. Murat, Evan Kiefl, Alon Shaiber, Iva Veseli, Samuel E. Miller, Matthew S. Schechter, Isaac Fink, Jessica N. Pan, Mahmoud Yousef, Emily C. Fogarty, Florian Trigodet, Andrea R. Watson, Özcan C. Esen, Ryan M. Moore, Quentin Clayssen, Michael D. Lee, Veronika Kivenson, Elaina D. Graham, Bryan D. Merrill, Antti Karkman, Daniel Blankenberg, John M. Eppley, Andreas Sjödin, Jarrod J. Scott, Xabier Vázquez-Campos, Luke J. McKay, Elizabeth A. McDaniel, Sarah L. R. Stevens, Rika E. Anderson, Jessika Fuessel, Antonio Fernandez-Guerra, Lois Maignien, Tom O. Delmont, and Amy D. Willis. 2021. “Community-Led, Integrated, Reproducible Multi-Omics with Anvi’o.” *Nature Microbiology* 6(1):3–6. doi:10.1038/s41564-020-00834-3.

Feng, Kai, Xi Peng, Zheng Zhang, Songsong Gu, Qing He, Wenli Shen, Zhujun Wang, Danrui Wang, Qiulong Hu, Yan Li, Shang Wang, and Ye Deng. 2022. “INAP: An Integrated Network Analysis Pipeline for Microbiome Studies.” *IMeta* 1(2). doi:10.1002/imt2.13.

Fontaine, Sébastien, Sébastien Barot, Pierre Barré, Nadia Bdioui, Bruno Mary, and Cornelia Rumpel. 2007. “Stability of Organic Carbon in Deep Soil Layers Controlled by Fresh Carbon Supply.” *Nature* 450(7167):277–80. doi:10.1038/nature06275.

Frioux, Clémence, Dipali Singh, Tamas Korcsmaros, and Falk Hildebrand. 2020. “From Bag-of-Genes to Bag-of-Genomes: Metabolic Modelling of Communities in the Era of Metagenome-Assembled Genomes.” *Computational and Structural Biotechnology Journal* 18:1722–34. doi:10.1016/j.csbj.2020.06.028.

Gallagher, John L., and F. Gerald Plumley. 1979. “UNDERGROUND BIOMASS PROFILES AND PRODUCTIVITY IN ATLANTIC COASTAL MARSHES.” *American Journal of Botany* 66(2):156–61. doi:10.1002/j.1537-2197.1979.tb06208.x.

Gibson, Scott M., Stephen P. Ficklin, Sven Isaacson, Feng Luo, Frank A. Feltus, and Melissa C. Smith. 2013. “Massive-Scale Gene Co-Expression Network Construction and Robustness Testing Using Random Matrix Theory.” *PLoS ONE* 8(2). doi:10.1371/journal.pone.0055871.

Guimond, Julia A., Angelia L. Seyfferth, Kevan B. Moffett, and Holly A. Michael. 2020. “A Physical-Biogeochemical Mechanism for Negative Feedback between Marsh Crabs and Carbon Storage.” *Environmental Research Letters* 15(3):034024. doi:10.1088/1748-9326/ab60e2.

Guimond, Julia, and Joseph Tamborski. 2021. “Salt Marsh Hydrogeology: A Review.” *Water* 13(4):543. doi:10.3390/w13040543.

Hou, Jialin, Yinzhao Wang, Pengfei Zhu, Na Yang, Lewen Liang, Tiantian Yu, Mingyang Niu, Kurt Konhauser, Ben J. Woodcroft, and Fengping Wang. 2023. “Taxonomic and Carbon Metabolic Diversification of Bathyarchaeia during Its Coevolution History with Early Earth Surface Environment.” *Science Advances* 9(27). doi:10.1126/sciadv.adf5069.

Howes, Brian L., John W. H. Dacey, and Gary M. King. 1984. “Carbon Flow through Oxygen and Sulfate Reduction Pathways in Salt Marsh Sediments1.” *Limnology and Oceanography* 29(5):1037–51. doi:10.4319/lo.1984.29.5.1037.

Inagaki, Fumio, Takuro Nunoura, Satoshi Nakagawa, Andreas Teske, Mark Lever, Antje Lauer, Masae Suzuki, Ken Takai, Mark Delwiche, Frederick S. Colwell, Kenneth H. Nealson, Koki Horikoshi, Steven D'Hondt, and Bo B. Jørgensen. 2006. "Biogeographical Distribution and Diversity of Microbes in Methane Hydrate-Bearing Deep Marine Sediments on the Pacific Ocean Margin." *Proceedings of the National Academy of Sciences* 103(8):2815–20. doi:10.1073/pnas.0511033103.

Jain, Chirag, Luis M. Rodriguez-R, Adam M. Phillippy, Konstantinos T. Konstantinidis, and Srinivas Aluru. 2018. "High Throughput ANI Analysis of 90K Prokaryotic Genomes Reveals Clear Species Boundaries." *Nature Communications* 9(1):5114. doi:10.1038/s41467-018-07641-9.

Jørgensen, Bo Barker, and Antje Boetius. 2007. "Feast and Famine — Microbial Life in the Deep-Sea Bed." *Nature Reviews Microbiology* 5(10):770–81. doi:10.1038/nrmicro1745.

Kirkpatrick, John B., Emily A. Walsh, and Steven D'Hondt. 2019. "Microbial Selection and Survival in Subseafloor Sediment." *Frontiers in Microbiology* 10. doi:10.3389/fmicb.2019.00956.

Kirwan, Matthew L., J. Patrick Megonigal, Genevieve L. Noyce, and Alexander J. Smith. 2023. "Geomorphic and Ecological Constraints on the Coastal Carbon Sink." *Nature Reviews Earth & Environment* 4(6):393–406. doi:10.1038/s43017-023-00429-6.

Kuzyakov, Yakov, and Evgenia Blagodatskaya. 2015. "Microbial Hotspots and Hot Moments in Soil: Concept & Review." *Soil Biology and Biochemistry* 83:184–99. doi:10.1016/j.soilbio.2015.01.025.

Langmead, Ben, and Steven L. Salzberg. 2012. "Fast Gapped-Read Alignment with Bowtie 2." *Nature Methods* 9(4):357–59. doi:10.1038/nmeth.1923.

Lever, Mark Alexander. 2012. "Acetogenesis in the Energy-Starved Deep Biosphere – A Paradox?" *Frontiers in Microbiology* 2. doi:10.3389/fmicb.2011.00284.

Li, Heng, Bob Handsaker, Alec Wysoker, Tim Fennell, Jue Ruan, Nils Homer, Gabor Marth, Goncalo Abecasis, and Richard Durbin. 2009. "The Sequence Alignment/Map Format and SAMtools." *Bioinformatics* 25(16):2078–79. doi:10.1093/bioinformatics/btp352.

Liang, Chao, Joshua P. Schimel, and Julie D. Jastrow. 2017. "The Importance of Anabolism in Microbial Control over Soil Carbon Storage." *Nature Microbiology* 2(8):17105. doi:10.1038/nmicrobiol.2017.105.

Liu, Jin-e, Rui-Ming Han, Hai-Rong Su, Ya-Ping Wu, Li-Min Zhang, Curtis J. Richardson, and Guo-Xiang Wang. 2017. "Effects of Exotic Spartina Alterniflora on Vertical Soil Organic Carbon Distribution and Storage Amount in Coastal Salt Marshes in Jiangsu, China." *Ecological Engineering* 106:132–39. doi:10.1016/j.ecoleng.2017.05.041.

Luo, Feng, Yunfeng Yang, Jianxin Zhong, Haichun Gao, Latifur Khan, Dorothea K. Thompson, and Jizhong Zhou. 2007. "Constructing Gene Co-Expression Networks and Predicting Functions of Unknown Genes by Random Matrix Theory." *BMC Bioinformatics* 8(1):299. doi:10.1186/1471-2105-8-299.

Moffett, Kevan B., Steven M. Gorelick, Robert G. McLaren, and Edward A. Sudicky. 2012. "Salt Marsh Ecohydrological Zonation Due to Heterogeneous Vegetation–Groundwater–Surface Water Interactions." *Water Resources Research* 48(2). doi:10.1029/2011WR010874.

Nayfach, Stephen, Simon Roux, Rekha Seshadri, Daniel Udwary, Neha Varghese, Frederik Schulz, Dongying Wu, David Paez-Espino, I. Min Chen, Marcel Huntemann, Krishna

Palaniappan, Joshua Ladau, Supratim Mukherjee, T. B. K. Reddy, Torben Nielsen, Edward Kirton, José P. Faria, Janaka N. Edirisinghe, Christopher S. Henry, Sean P. Jungbluth, Dylan Chivian, Paramvir Dehal, Elisha M. Wood-Charlson, Adam P. Arkin, Susannah G. Tringe, Axel Visel, Helena Abreu, Silvia G. Acinas, Eric Allen, Michelle A. Allen, Lauren V. Alteio, Gary Andersen, Alexandre M. Anesio, Graeme Attwood, Viridiana Avila-Magaña, Yacine Badis, Jake Bailey, Brett Baker, Petr Baldrian, Hazel A. Barton, David A. C. Beck, Eric D. Becraft, Harry R. Beller, J. Michael Beman, Rizlan Bernier-Latmani, Timothy D. Berry, Anthony Bertagnolli, Stefan Bertilsson, Jennifer M. Bhatnagar, Jordan T. Bird, Jeffrey L. Blanchard, Sara E. Blumer-Schuette, Brendan Bohannan, Mikayla A. Borton, Allyson Brady, Susan H. Brawley, Juliet Brodie, Steven Brown, Jennifer R. Brum, Andreas Brune, Donald A. Bryant, Alison Buchan, Daniel H. Buckley, Joy Buongiorno, Hinsby Cadillo-Quiroz, Sean M. Caffrey, Ashley N. Campbell, Barbara Campbell, Stephanie Carr, Jo Lynn Carroll, S. Craig Cary, Anna M. Cates, Rose Ann Cattolico, Ricardo Cavicchioli, Ludmila Chistoserdova, Maureen L. Coleman, Philippe Constant, Jonathan M. Conway, Walter P. Mac Cormack, Sean Crowe, Byron Crump, Cameron Currie, Rebecca Daly, Kristen M. DeAngelis, Vincent Denef, Stuart E. Denman, Adey Desta, Hebe Dionisi, Jeremy Dodsworth, Nina Dombrowski, Timothy Donohue, Mark Dopson, Timothy Driscoll, Peter Dunfield, Christopher L. Dupont, Katherine A. Dynarski, Virginia Edgcomb, Elizabeth A. Edwards, Mostafa S. Elshahed, Israel Figueroa, Beverly Flood, Nathaniel Fortney, Caroline S. Fortunato, Christopher Francis, Claire M. M. Gachon, Sarahi L. Garcia, Maria C. Gazitua, Terry Gentry, Lena Gerwick, Javad Gharechahi, Peter Girguis, John Gladden, Mary Gradoville, Stephen E. Grasby, Kelly Gravuer, Christen L. Grettenberger, Robert J. Gruninger, Jiarong Guo, Mussie Y. Habteselassie, Steven J. Hallam, Roland Hatzenpichler, Bela Hausmann, Terry C. Hazen, Brian Hedlund, Cynthia Henny, Lydie Herfort, Maria Hernandez, Olivia S. Hershey, Matthias Hess, Emily B. Hollister, Laura A. Hug, Dana Hunt, Janet Jansson, Jessica Jarett, Vitaly V. Kadnikov, Charlene Kelly, Robert Kelly, William Kelly, Cheryl A. Kerfeld, Jeff Kimbrel, Jonathan L. Klassen, Konstantinos T. Konstantinidis, Laura L. Lee, Wen Jun Li, Andrew J. Loder, Alexander Loy, Mariana Lozada, Barbara MacGregor, Cara Magnabosco, Aline Maria da Silva, R. Michael McKay, Katherine McMahon, Chris S. McSweeney, Mónica Medina, Laura Meredith, Jessica Mizzi, Thomas Mock, Lily Momper, Mary Ann Moran, Connor Morgan-Lang, Duane Moser, Gerard Muyzer, David Myrold, Maisie Nash, Camilla L. Nesbø, Anthony P. Neumann, Rebecca B. Neumann, Daniel Noguera, Trent Northen, Jeanette Norton, Brent Nowinski, Klaus Nüsslein, Michelle A. O'Malley, Rafael S. Oliveira, Valeria Maia de Oliveira, Tullis Onstott, Jay Osvatic, Yang Ouyang, Maria Pachiadaki, Jacob Parnell, Laila P. Partida-Martinez, Kabir G. Peay, Dale Pelletier, Xuefeng Peng, Michael Pester, Jennifer Pett-Ridge, Sari Peura, Petra Pjevac, Alvaro M. Plominsky, Anja Poehlein, Phillip B. Pope, Nikolai Ravin, Molly C. Redmond, Rebecca Reiss, Virginia Rich, Christian Rinke, Jorge L. Mazza Rodrigues, William Rodriguez-Reillo, Karen Rossmassler, Joshua Sackett, Ghasem Hosseini Salekdeh, Scott Saleska, Matthew Scarborough, Daniel Schachtman, Christopher W. Schadt, Matthew Schrenk, Alexander Sczyrba, Aditi Sengupta, Joao C. Setubal, Ashley Shade, Christine Sharp, David H. Sherman, Olga V. Shubenkova, Isabel Natalia Sierra-Garcia, Rachel Simister, Holly Simon, Sara Sjöling, Joan Slonczewski, Rafael Soares Correa de Souza, John R. Spear, James C. Stegen, Ramunas Stepanauskas, Frank Stewart, Garret Suen, Matthew Sullivan, Dawn Sumner, Brandon K. Swan, Wesley Swingley, Jonathan Tarn,

865 Gordon T. Taylor, Hanno Teeling, Memory Tekere, Andreas Teske, Torsten Thomas,
866 Cameron Thrash, James Tiedje, Claire S. Ting, Benjamin Tully, Gene Tyson, Osvlado Ulloa,
867 David L. Valentine, Marc W. Van Goethem, Jean VanderGheynst, Tobin J. Verbeke, John
868 Vollmers, Aurèle Vuillemin, Nicholas B. Waldo, David A. Walsh, Bart C. Weimer, Thea
869 Whitman, Paul van der Wielen, Michael Wilkins, Timothy J. Williams, Ben Woodcroft,
870 Jamie Woolet, Kelly Wrighton, Jun Ye, Erica B. Young, Noha H. Youssef, Feiqiao Brian Yu,
871 Tamara I. Zemskaya, Ryan Ziels, Tanja Woyke, Nigel J. Mouncey, Natalia N. Ivanova, Nikos
872 C. Kyrpides, and Emiley A. Eloe-Fadrosh. 2021. "A Genomic Catalog of Earth's
873 Microbiomes." *Nature Biotechnology* 39(4):499–509. doi:10.1038/s41587-020-0718-6.
874 Newman, M. E. J. 2004. "Fast Algorithm for Detecting Community Structure in Networks."
875 *Physical Review E* 69(6):066133. doi:10.1103/PhysRevE.69.066133.
876 Olesen, Jens M., Jordi Bascompte, Yoko L. Dupont, and Pedro Jordano. 2006. "The Smallest of
877 All Worlds: Pollination Networks." *Journal of Theoretical Biology* 240(2):270–76.
878 doi:10.1016/j.jtbi.2005.09.014.
879 Olm, Matthew R., Christopher T. Brown, Brandon Brooks, and Jillian F. Banfield. 2017. "DRep: A
880 Tool for Fast and Accurate Genomic Comparisons That Enables Improved Genome
881 Recovery from Metagenomes through de-Replication." *The ISME Journal* 11(12):2864–68.
882 doi:10.1038/ismej.2017.126.
883 Parks, Donovan H., Michael Imelfort, Connor T. Skennerton, Philip Hugenholtz, and Gene W.
884 Tyson. 2015. "CheckM: Assessing the Quality of Microbial Genomes Recovered from
885 Isolates, Single Cells, and Metagenomes." *Genome Research* 25(7):1043–55.
886 doi:10.1101/gr.186072.114.
887 Payne, Paige E., Loren N. Knobbe, Patricia Chanton, Julian Zaugg, Behzad Mortazavi, and Olivia
888 U. Mason. 2025. "Uncovering Novel Functions of the Enigmatic, Abundant, and Active
889 *Anaerolineae* in a Salt Marsh Ecosystem." *MSystems* 10(1). doi:10.1128/msystems.01162-
890 24.
891 Petro, C., P. Starnawski, A. Schramm, and KU Kjeldsen. 2017. "Microbial Community Assembly
892 in Marine Sediments." *Aquatic Microbial Ecology* 79(3):177–95. doi:10.3354/ame01826.
893 Petro, Caitlin, Birthe Zäncker, Piotr Starnawski, Lara M. Jochum, Timothy G. Ferdelman, Bo
894 Barker Jørgensen, Hans Røy, Kasper U. Kjeldsen, and Andreas Schramm. 2019. "Marine
895 Deep Biosphere Microbial Communities Assemble in Near-Surface Sediments in Aarhus
896 Bay." *Frontiers in Microbiology* 10. doi:10.3389/fmicb.2019.00758.
897 Porter, Abigail W., and Lily Y. Young. 2014. "Benzoyl-CoA, a Universal Biomarker for Anaerobic
898 Degradation of Aromatic Compounds." Pp. 167–203 in.
899 Qiu, Yan-Ling, Satoshi Hanada, Akiyoshi Ohashi, Hideki Harada, Yoichi Kamagata, and Yuji
900 Sekiguchi. 2008. "*Syntrophorhabdus Aromaticivorans* Gen. Nov., Sp. Nov., the First
901 Cultured Anaerobe Capable of Degrading Phenol to Acetate in Obligate Syntrophic
902 Associations with a Hydrogenotrophic Methanogen." *Applied and Environmental*
903 *Microbiology* 74(7):2051–58. doi:10.1128/AEM.02378-07.
904 Qiu, Yan-Ling, Yuji Sekiguchi, Satoshi Hanada, Hiroyuki Imachi, I. Cheng Tseng, Sheng-Shung
905 Cheng, Akiyoshi Ohashi, Hideki Harada, and Yoichi Kamagata. 2006. "Pelotomaculum
906 Terephthalicum Sp. Nov. and Pelotomaculum Isophthalicum Sp. Nov.: Two Anaerobic
907 Bacteria That Degrade Phthalate Isomers in Syntrophic Association with Hydrogenotrophic
908 Methanogens." *Archives of Microbiology* 185(3):172–82. doi:10.1007/s00203-005-0081-5.

R Foundation for Statistical Computing, Vienna, Austria. 2021. “R: A Language and Environment for Statistical Computing.”

Seitz, Kiley W., Cassandre S. Lazar, Kai-Uwe Hinrichs, Andreas P. Teske, and Brett J. Baker. 2016. “Genomic Reconstruction of a Novel, Deeply Branched Sediment Archaeal Phylum with Pathways for Acetogenesis and Sulfur Reduction.” *The ISME Journal* 10(7):1696–1705. doi:10.1038/ismej.2015.233.

Shannon, Paul, Andrew Markiel, Owen Ozier, Nitin S. Baliga, Jonathan T. Wang, Daniel Ramage, Nada Amin, Benno Schwikowski, and Trey Ideker. 2003. “Cytoscape: A Software Environment for Integrated Models of Biomolecular Interaction Networks.” *Genome Research* 13(11):2498–2504. doi:10.1101/gr.1239303.

Spivak, Amanda C., Jonathan Sanderman, Jennifer L. Bowen, Elizabeth A. Canuel, and Charles S. Hopkinson. 2019. “Global-Change Controls on Soil-Carbon Accumulation and Loss in Coastal Vegetated Ecosystems.” *Nature Geoscience* 12(9):685–92. doi:10.1038/s41561-019-0435-2.

Stewart, Robert D., Marc D. Auffret, Amanda Warr, Andrew H. Wiser, Maximilian O. Press, Kyle W. Langford, Ivan Liachko, Timothy J. Snelling, Richard J. Dewhurst, Alan W. Walker, Rainer Roehe, and Mick Watson. 2018. “Assembly of 913 Microbial Genomes from Metagenomic Sequencing of the Cow Rumen.” *Nature Communications* 9(1):1–11. doi:10.1038/s41467-018-03317-6.

Tebbe, Dennis Alexander, Simone Geihser, Bernd Wemheuer, Rolf Daniel, Hendrik Schäfer, and Bert Engelen. 2022. “Seasonal and Zonal Succession of Bacterial Communities in North Sea Salt Marsh Sediments.” *Microorganisms* 10(5):859. doi:10.3390/microorganisms10050859.

Tobias, Craig, and Scott C. Neubauer. 2018. “Salt Marsh Biogeochemistry-An Overview.” Pp. 539–96 in *Coastal Wetlands: An Integrated Ecosystem Approach*. Elsevier.

Vekeman, Bram, Frederiek-Maarten Kerckhof, Geert Cremers, Paul de Vos, Peter Vandamme, Nico Boon, Huub J. M. Op den Camp, and Kim Heylen. 2016. “New *Methyloceanibacter* Diversity from North Sea Sediments Includes Methanotroph Containing Solely the Soluble Methane Monooxygenase.” *Environmental Microbiology* 18(12):4523–36. doi:10.1111/1462-2920.13485.

Vineis, Joseph H., Ashley N. Bulseco, and Jennifer L. Bowen. 2023. “Microbial Chemolithoautotrophs Are Abundant in Salt Marsh Sediment Following Long-Term Experimental Nitrate Enrichment.” *FEMS Microbiology Letters* 370. doi:10.1093/femsle/fnad082.

Walsh, Emily A., John B. Kirkpatrick, Scott D. Rutherford, David C. Smith, Mitchell Sogin, and Steven D’Hondt. 2016. “Bacterial Diversity and Community Composition from Seasurface to Subseafloor.” *The ISME Journal* 10(4):979–89. doi:10.1038/ismej.2015.175.

Wang, Miao, Erqin Li, Chen Liu, Alexandre Jousset, and Joana F. Salles. 2017. “Functionality of Root-Associated Bacteria along a Salt Marsh Primary Succession.” *Frontiers in Microbiology* 8. doi:10.3389/fmicb.2017.02102.

Whelan, Simon, and Nick Goldman. 2001. “A General Empirical Model of Protein Evolution Derived from Multiple Protein Families Using a Maximum-Likelihood Approach.” *Molecular Biology and Evolution* 18(5):691–99. doi:10.1093/oxfordjournals.molbev.a003851.

Xiao, Kai, Alicia M. Wilson, Hailong Li, and Carolyn Ryan. 2019. “Crab Burrows as Preferential Flow Conduits for Groundwater Flow and Transport in Salt Marshes: A Modeling Study.” *Advances in Water Resources* 132:103408. doi:10.1016/j.advwatres.2019.103408.

Yao, Zhiyuan, Shicong Du, Chunling Liang, Yueji Zhao, Francisco Dini-Andreote, Kai Wang, and Demin Zhang. 2019. “Bacterial Community Assembly in a Typical Estuarine Marsh with Multiple Environmental Gradients.” *Applied and Environmental Microbiology* 85(6). doi:10.1128/AEM.02602-18.

Yu, Tiantian, Weichao Wu, Wenyue Liang, Mark Alexander Lever, Kai-Uwe Hinrichs, and Fengping Wang. 2018. “Growth of Sedimentary Bathyarchaeota on Lignin as an Energy Source.” *Proceedings of the National Academy of Sciences* 115(23):6022–27. doi:10.1073/pnas.1718854115.

Zhou, Zhichao, Patricia Q. Tran, Adam M. Breister, Yang Liu, Kristopher Kieft, Elise S. Cowley, Ulas Karaoz, and Karthik Anantharaman. 2022. “METABOLIC: High-Throughput Profiling of Microbial Genomes for Functional Traits, Metabolism, Biogeochemistry, and Community-Scale Functional Networks.” *Microbiome* 10(1):33. doi:10.1186/s40168-021-01213-8.

Zimmermann, Johannes, Christoph Kaleta, and Silvio Waschina. 2021. “Gapseq: Informed Prediction of Bacterial Metabolic Pathways and Reconstruction of Accurate Metabolic Models.” *Genome Biology* 22(1):81. doi:10.1186/s13059-021-02295-1.